universität wien

DIPLOMARBEIT

Titel der Diplomarbeit

Functional Analysis of the *Escherichia coli* Hfq_{G29A} Variant

angestrebter akademischer Grad

Magister der Naturwissenschaften (Mag. rer.nat.)

Verfasserin / Verfasser:	Hermann Hämmerle
Matrikel-Nummer:	0202546
Studienrichtung /Studienzweig (lt. Studienblatt):	A-441
Betreuerin / Betreuer:	Prof. Dr. Udo Bläsi

Wien, am 22.06.2009

Contents

1 ABSTRACT

The RNA chaperone Hfq is conserved throughout Gram-positive and Gram-negative bacteria. Several functional studies on the hexameric *E. coli* Hfq protein revealed two distinct binding sites for RNA. The proximal site preferably binds non-coding RNA (ncRNA), whereas the distal site binds poly(A) tails. A recent NMR study suggested that Hfq_{Gly29} displayed a rather high flexibility when compared to other amino acids in the N-terminal region of Hfq. In this study, the effect of a missense mutation, changing glycine at position 29 to alanine, was studied. Gel-shift experiments showed that the mutant Hfq_{G29A} protein was able to bind mRNA and ncRNA, and biochemical experiments confirmed that Hfq_{G29A} was functional in facilitating the annealing of the ncRNA DsrA with *rpoS* mRNA, which is required for translation initiation of *rpoS* at low temperatures. However, western-blot analysis revealed that the hfq_{G29A} strain AM111 (pAHG29A), grown at 25 °C, had strongly reduced levels of RpoS protein comparable to an hfq^- strain. Bandshift competition assays suggested that Hfq_{G29A} is defective in the displacement of the protein from the DsrA-*rpoS*-Hfq complex, which may explain why Hfq_{G29A} failed to stimulate *rpoS* translation.

2 ZUSAMMENFASSUNG

Das RNA Chaperon Hfq ist in Gram-positiven und in Gram-negativen Bakterien konserviert. Mehrere funktionelle Studien über das hexamere *E. coli* Hfq Protein ließen zwei verschieden Bindungsseiten für RNA erkennen. Die proximale Seite bindet bevorzugt nicht-kodierende RNA (ncRNA), während die distale Seite poly(A) bindet. In einer kürzlichen NMR Studie wurde gezeigt, dass Hfq_{Gly29} im Vergleich mit anderen N-terminalen Aminosäuren eine hohe Flexibilität aufweist. In dieser Studie wurde der Effekt einer „missense mutation" untersucht bei der Glycin in Position 29 zu Alanin ausgetauscht wurde. Gel-shift Experimente zeigten, dass das mutierte Hfq_{G29A} Protein in der Lage war mRNA und ncRNA zu binden und biochemische Untersuchungen belegten, dass Hfq_{G29A} die Interaktion der ncRNA DsrA und *rpoS* mRNA stimulierte. Im Gegensatz dazu zeigten Western-Blot Analysen, dass der *hfq*$_{G29A}$ Stamm AM111 (pAHG29A) vergleichbar reduzierte Werte an RpoS Protein aufwies wie ein *hfq*$^-$ Stamm. Kompetitionsexperimente deuteten darauf hin, dass Hfq_{G29A} einen Defekt in der Dissoziation von dem DsrA-*rpoS*-Hfq Komplex aufweist, was wiederum den Defekt von Hfq_{G29A} in der Stimulierung der *rpoS* Translation erklären könnte.

3 INTRODUCTION

3.1 Hfq structure and function

The *Escherichia coli* host factor I/Q (Hfq) protein was first described as a factor necessary for replication of the RNA plus-strand of bacteriophage Qβ (1,2). An *hfq* insertion mutation was shown to cause broadly pleiotropic phenotypes including decreased growth, increased cell size, osmosensitivity, increased oxidation of carbon sources and sensitivity to ultraviolet light, suggesting that Hfq plays a global role in *Escherichia coli* physiology (3). Subsequent phylogenetic analysis revealed that out of 58 completed and 82 unfinished bacterial genomes approximately half contain at least one gene that codes for Hfq orthologues (Figure 1) (4).

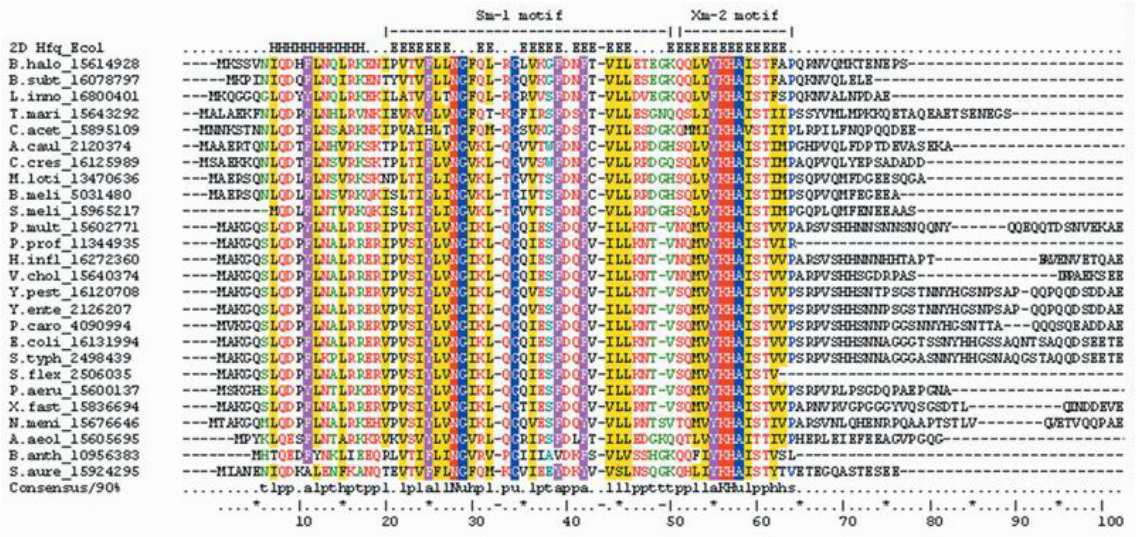

Figure 1. Multiple alignment of Hfq proteins from 26 bacterial genomes. Predicted secondary structure for Hfq proteins is shown above the corresponding sequences: H, α-helix; E, β-strand. The Sm1 and Xm2 motifs of Hfq proteins are shown. The 90% consensus shown below the alignment was derived using the following amino acid groupings. Positively charged residues (RKH) are shown as white letters on a red background; polar residues (p, KRHEDQNST) are shown as red letters; turn-like residues (t, ACDEGKNQRST) are green letters; bulky hydrophobic residues (h, ACLIVMHYFW) and the aliphatic subset of these type residues (l, LIVM) have a yellow background; aromatic residues (a, FHWY) are white letters with a purple background; small residues (s, ACDGNPSTV) are blue letters; tiny (u, AGS) are white letters with a blue background. Sequences are denoted by the species abbreviation followed by GI number. Species abbreviations: M.ther, *M. thermoautotrophicum*; B.halo, *Bacillus halodurans*; B.subt, *Bacillus subtilis*; L.inno, *Listeria innocua*; T.mari, *Thermotoga maritima*; C.acet, *Clostridium acetobutylicum*; A.caul, *Azorhizobium caulinodans*; C.cres, *Caulobacter crescentus*; M.loti,

Mesorhizobium loti; B.meli, *Brucella melitensis biovar Abortus*; S.meli, *Sinorhizobium meliloti*; P.mult, *Pasteurella multocida*; P.prof, *Photobacterium profundum*; H.infl, *Haemophilus influenzae*; V.chol, *Vibrio cholerae*; Y.pest, *Yersinia pestis*; Y.ente, *Yersinia enterocolitica*; P.caro, *Pectobacterium carotovorum*; E.coli, *E.coli*; S.typh, *Salmonella typhimurium*; S.flex, *Shigella flexneri*; P.aeru, *P. aeruginosa*; X.fast, *Xylella fastidiosa*; N.meni, *Neisseria meningitidis*; A.aeol, *Aquifex aeolicus*; B.anth, *Bacillus anthracis*; S.aure, *S. aureus* (4).

The *E. coli hfq* gene is part of the *amiB-mutL-miaA-hfq-hflX* super-operon, whose transcription is complex and driven by several promoters (3). In exponentially growing cells the synthesis rate of Hfq was shown to be increased when compared to stationary phase (5). However, it has also been reported that the total concentration of Hfq is higher in slow growing cells (6), and upon entry into stationary phase (7). Hfq interacts with small non-coding RNAs (ncRNAs) and assists in ncRNA-mRNA annealing, which can result in post-transcriptional gene activation or silencing (8-11). Since Hfq plays an important role in regulation of stress responses, the higher abundance of Hfq in stationary phase can be rationalized in light of an increased expression of ncRNAs, for many of which Hfq is required for riboregulation (12,13). Six Hfq monomers form one homo-hexameric protein. Up to 10.000 hexameric molecules of Hfq are present per cell, which corresponds to an intracellular concentration of ~15 μM (5-7). Since this value is 500-fold to 1000-fold higher than the dissociation constant of Hfq for small A/U-rich oligonucleotides and for Spot 42 RNA, respectively, much of the intracellular Hfq should be bound to cellular RNA (14-16). Consistent with this, the majority (80-90%) seems to be loosely associated with ribosomes and can be washed off by salt. A significant amount of Hfq (10-20%) was also found in the bacterial nucleoid (5,17).

All Hfq proteins are characterized by an N-terminal α-helix followed by five β-strands that display the topology β5α1β1β2β3β4 (18). The *E. coli* Hfq consists of 102 amino acid residues (11.2 kDa) and forms a heat-stable, homo-hexameric, ring-shaped structure with a central cavity (15,19,20) (Figure 2). The hexamer is formed by interactions of β4 from one monomer with β5 from its neighbouring subunit. Studies on the crystal structure of an *E. coli* Hfq protein encompassing amino acids 1-72 by Sauter *et al.* (2003) and on the

crystal structure of *S. aureus* Hfq by Schumacher *et al.* (2002) suggested that the ring has an outer diameter of ~70 Å and a thickness of ~25 Å while the central pore is 8 Å to 12 Å in width (9,16,19).

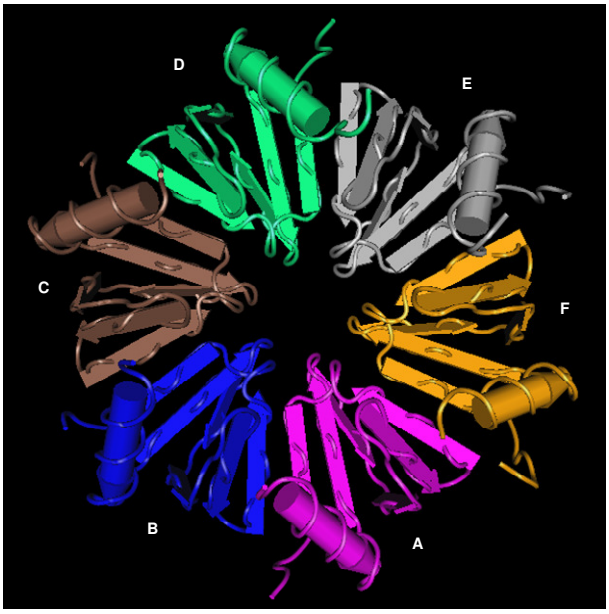

Figure 2. Crystal Structure of *E. coli* Hfq. Proximal face representation of the Hfq hexamer. The six domains comprising the hexameric protein are depicted in different colours. β-sheets are represented as flat arrows, α-helices as tubes. Residues 7-68 are observed in all six subunits and additional residues were modelled at the N-terminus and the C-terminus (from Gly4 in monomers D and E, and up to His71 in F) (19).

3.2 Hfq – a Sm-like protein

Electron microscopy and crystallographic studies on Hfq revealed a structure which is similar to that of Sm and Sm-like proteins which contain heat-stable β-sheets (4,16,19,21,22). Another hallmark of bacterial Sm-proteins is the formation of hexamers (4,19,23). In contrast, eukaryotic Sm-proteins form rings composed of seven different subunits (24), whereas archaeal Sm-proteins form rings with either seven (25-27) or six identical subunits (23). Eukaryotic Sm-proteins are involved in pre-mRNA splicing, mRNA stability and translation (28,29) and bind to various RNAs by recognizing short U-rich stretches (25). The regions of Sm and Lsm proteins shown to contact RNA are defined by the conservation of two sequence motifs that encompass the loops, the Sm1 and Sm2 motif which are separated by a region of variable length and sequence (30,31). An alignment between bacterial Hfq-homologues and Sm-proteins

revealed that many of the residues conserved in the Sm1 motif are conserved in the bacterial Hfq proteins (9) (Figure 3). In Hfq, the Sm1 motif comprises β-strands 1-3 and shares a conserved pattern of hydrophobic residues as well as a highly conserved acidic residue (Asp40 in Hfq) with Sm-proteins (16). The homology between the Sm2 motif in Sm-proteins and Hfq is less obvious. However, Hfq proteins possess a second region of high conservation containing a number of hydrophobic residues found in the conserved Sm2 sequence motif of Sm-proteins (9). This "Hfq Sm2 motif" spans β-sheets 4 and 5 and comprises the highly conserved amino acid sequence YKHAI in loop 5 (YKHAI motif in bacteria) (19) (Figure 3).

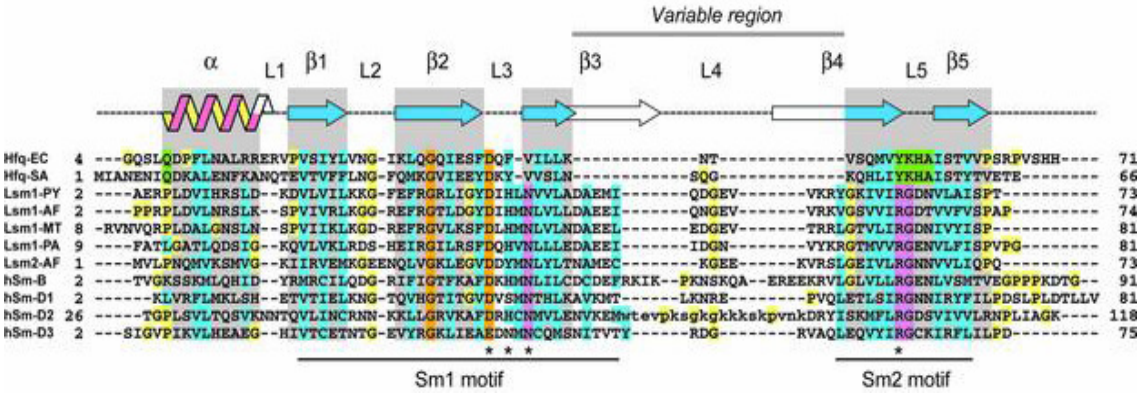

Figure 3. The structure-based sequence alignment is confined to the regions revealed by crystallographic studies (first and last observed residues are indicated on the left- and right-sites of the corresponding sequences). Gray boxes highlight the common backbone regions defining a minimal Sm-fold. Overall conserved residues appear in orange, those specific for the Hfq family are in green and those characteristic to Archaea and Eukaryotes are in magenta. Blue boxes indicate conserved patches of aliphatic or aromatic residues. The residues in loops L3 and L5 that form the NBP in the structures of Lsm–RNA complexes are indicated by stars. The residues belonging to loop L4 are separated from the adjacent β-strands by gaps to highlight the variability of this region (19).

Like Sm and Lsm proteins, Hfq is able to bind RNA and both Hfq and Sm/Lsm rings exhibit central nucleotide binding pockets (NBPs) (19,24,25,32,33). In Hfq the loops 3 and 5 from individual subunits form a NBP consisting of almost universally conserved residues (19) (Figure 3). The protein binds to RNAs preferably at A/U-rich regions preceded or followed by a stem-loop structure (10,34-36). The X-ray structure of *S. aureus* Hfq in complex with the single-

stranded hepta-oligoribonucleotide, AU_5G, revealed a circular binding mode of the RNA within the central basic pore of Hfq (Figure 4) (16).

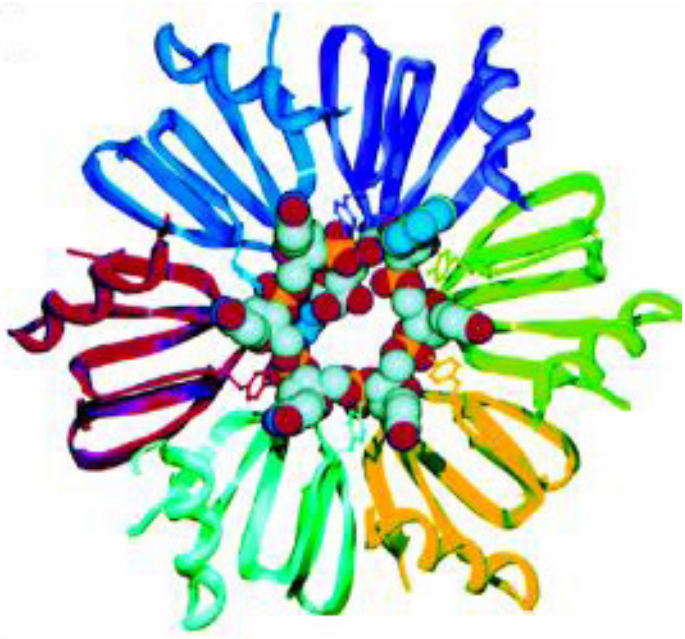

Figure 4. Ribbon diagram of *S. aureus* Hfq–RNA complex with the RNA represented as a CPK model. The oxygen, nitrogen, carbon and phosphorus atoms of the RNA are coloured red, blue, gray and yellow, respectively. Also shown as balls and sticks are the Tyr42 residues from each subunit, which stack with the RNA bases (16).

3.3 Hfq in riboregulation

Hfq facilitates the interaction between ncRNAs and mRNAs. This interaction can either result in opening of a secondary structure, which interferes with translation initiation or in ncRNA binding to the ribosome binding site, thereby preventing translation initiation (8-10,15,18,37-39). Several studies revealed that in *E. coli* Hfq interacts with over a dozen ncRNAs and mRNAs thereby activating (e.g. DsrA/*rpoS* and RprA/*rpoS*) (8,11) or repressing (e.g. OxyS/*rpoS* and RyhB/*sodB*) (9,10) translation of different mRNAs.

Binding of Hfq affects the stability of several mRNAs (7,40,41) and ncRNAs (8,42-44). It was shown that Hfq stimulates *ompA* mRNA decay by interfering with ribosome binding (40) and that it protects the ncRNA RyhB from degradation by RNase E (42). Moreover, the ncRNAs RyhB, DsrA and OxyS were degraded more rapidly in the absence of rifampicin than in its presence, suggesting that these small RNAs are also degraded as a consequence of base-

pairing with their mRNA targets (42). RNase E is necessary for degradation of RyhB in the absence of Hfq and for the degradation of RyhB when it is acting as a riboregulator. Thus, it seems possible that Hfq binding directly blocks RNase E access to RyhB. It is striking, that the recognition sites of Hfq and RNase E are overlapping. The Hfq binding motif on RNAs is A/U-rich as is the recognition sequence of RNase E (9,15,16,34,42,45-47).

3.4 Hfq RNA chaperone activity

RNA chaperones are proteins involved in RNA folding and, in contrast to RNA-binding proteins, are defined by their transient action (35). RNA chaperones prevent misfolding, resolve misfolded RNA structures (48) or catalyze annealing of complementary nucleic acids (49). Hfq was shown to stimulate group I intron splicing in an *in vivo* RNA-chaperone assay (35,50). Binding of Hfq to *ompA* mRNA in the vicinity of the ribosome binding site (RBS) affected the structure of the RBS. In addition, toeprinting studies revealed that the Hfq-induced structural changes in *ompA* RNA, which impeded 30S binding, are maintained after removal of the protein (35).

Fluorescence resonance energy transfer assays (FRET) corroborated the RNA chaperone activity of Hfq (51). It was shown that Hfq binds rapidly to both *rpoS* and DsrA and melts the stem of *rpoS* (average reaction time ~4 min). The increased local concentration of DsrA and the dissociation of the intramolecular secondary structure at the 5' end of *rpoS* facilitate the annealing between *rpoS* and DsrA (average reaction time ~9 min). Although Hfq has been reported to have ATPase activity (52), such an activity does not appear to be necessary for its RNA chaperone functions in sequence-specific RNA annealing or melting (51).

3.5 Hfq binding sites for RNA

Several studies on Hfq missense mutants with altered RNA binding capacity and functionality suggested two distinct RNA binding sites located on the Hfq homohexamer. The proximal site preferably binds ncRNA, whereas the distal site binds poly(A) tails (53-56). In addition to the known binding cavity along the inner rim comprising six separate, but linked potential nucleotide-binding pockets (16), the proximal amino acid residues Y55, K56 and H57 were shown to be involved in poly-(U) binding (53) (Figure 5). Replacement of the amino acids R16, F39 (54), Y55 and K56 (53) resulted in reduced affinity for the ncRNA DsrA and mutation of V43 negatively affected binding of 3'-*rpsO*-(A)18 and *hfq*(101) mRNA (55) (Figure 5). Interestingly, the Hfq protein showed a 3-fold reduced affinity for A_{27} when the proximal amino acid Y55 was changed to alanine (53). Mutations of amino acids Y25, I30 and K31 on the distal site of the hexamer resulted in a less efficient binding of poly(A) RNA (53,54,56).

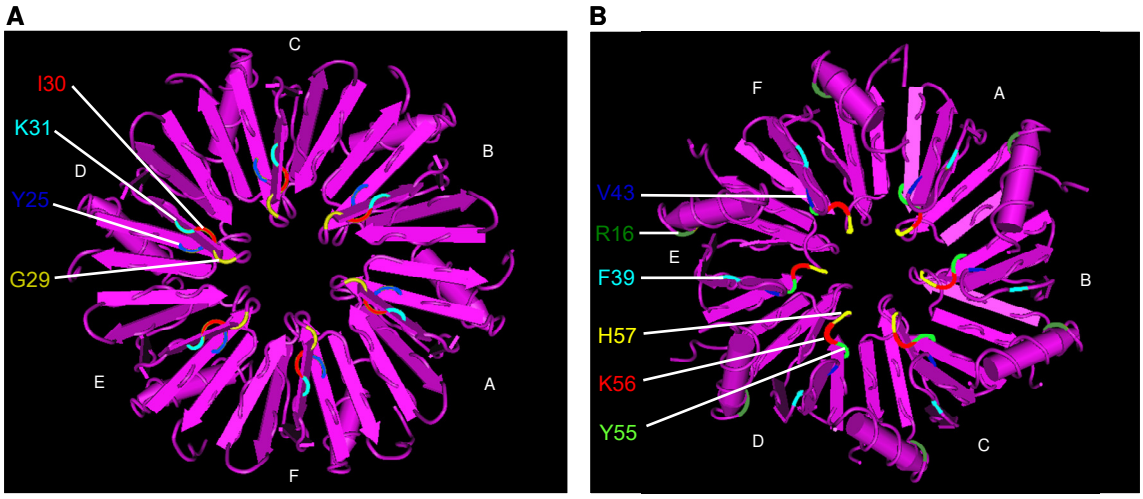

Figure 5. Amino acids that contribute to RNA binding are shown in the 3D structure of *E. coli* Hfq. **(A)** Distal site of the Hfq hexamer. Tyr25 is shown in blue, Gly29 in yellow, Ile30 in red and Lys31 in turquoise. **(B)** Proximal site of the Hfq hexamer. Arg16 is highlighted in dark green, Phe39 in turquoise, Val43 in blue, Tyr55 in bright green, Lys56 in red and His57 in yellow. Residues 7-68 are observed in all six subunits and additional residues were modelled at the N-terminus and the C-terminus (from Gly4 in monomers D and E, and up to His71 in F) (19).

A C-terminally truncated variant of Hfq (Hfq_{65}), comprising the conserved hexameric core of Hfq, was shown to be defective in auto- and riboregulation (57). Although Hfq_{65} retained the capacity to bind ncRNAs, and, as evident from fluorescence resonance energy transfer assays (FRET), to induce structural changes in the ncRNA DsrA, the truncated variant was unable to accommodate two non-complementary RNA oligonucleotides, and was defective in mRNA binding. These studies indicate that the C-terminal extension of *E. coli* Hfq constitutes a hitherto unrecognized RNA interaction surface with specificity for mRNAs (57).

3.6 Hfq ATPase activity

Sukhodolets and Garges (2003) reported an ATPase activity for Hfq (52). The N-terminal part of Hfq shows homology to the part of the heat-shock protein ClpB that had been identified as an ATP-binding site (58), which includes the Walker A box, a hallmark for ATP-binding proteins (52) (Figure 6).

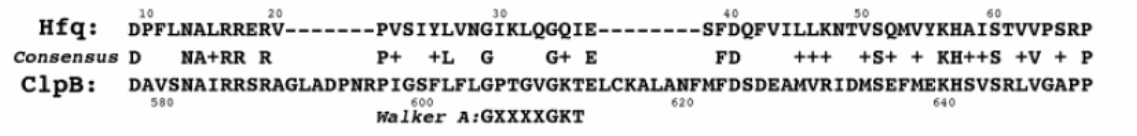

Figure 6. The alignment shows homology between Hfq and the part of the heat-shock protein ClpB that has been identified as the ATP-binding site (52).

Arluison *et al.* (2007) studied the effect of ATP on Hfq-RNA complexes and established Hfq as an ATP-binding protein (56). In this study it was proposed that an ATP-binding site is located near the outer rim, at the "L4" face of the doughnut-shaped Hfq molecule, comprising the highly conserved amino acids Tyr25, Gln52 (forming the putative ATP-binding pocket) and Lys31 (located within the putative Walker A box). It was shown that a replacement of Tyr25 – the amino acid forming one of the "walls" of the predicted ATP-binding cleft – resulted in reduced ATP binding and reduced ATP hydrolysis. Moreover, an

electron microscopic analysis revealed that the ternary RNA-Hfq-ATP complex is structurally different from the RNA-Hfq, Hfq-nucleotide, or RNA-Hfq-non-hydrolysable ATP analogue complexes. The data indicated that binding of both RNA and ATP is accompanied by a detectable distortion in the Hfq sixfold symmetry as shape influences rotational motions. Consistent with this is the observed change in fluorescence anisotropy in Hfq-RNA complexes in the presence of ATP (56). In addition, binding studies with 5'-fluoresceinated RNAs, RNA footprinting and electrophoretic mobility shift assays indicated dissociation of Hfq-RNA complexes in the presence of ATP (56).

3.7 The DsrA/*rpoS* paradigm

One of the best studied activities of Hfq is the DsrA-mediated stimulation of *rpoS* expression. The *rpoS* gene encodes the stationary phase/stress sigma factor RpoS (σ^S), which can replace the house-keeping sigma factor σ^{70} (RpoD) under stress conditions (59). The RpoS regulon includes genes encoding products involved in functions as diverse as general stress resistance (UV, hyperosmolarity, acid shock, oxidative and temperature stresses), carbon metabolism, cell envelope and morphology (60). The *rpoS* mRNA forms a complex secondary structure in which the translational initiation region (TIR) within the 5'-untranslated region is sequestered and therefore not accessible for ribosomes (59). Three ncRNAs were found to be involved in regulation of *rpoS* translation: DsrA and RprA are able to activate *rpoS* expression by base-pairing with the *rpoS* leader (61), whereas the ncRNA OxyS interacts with *rpoS* mRNA and prevents translation (9,62). All three ncRNAs require Hfq for activity (8,63,64). Sledjeski *et al.* (1996) reported that *rpoS* expression is low during exponential phase at temperatures of 30°C and above. However, at 20°C substantial synthesis of RpoS was observed during exponential growth, which was dependent on the 87nt DsrA RNA. The expression of *dsrA* is increased at low temperatures (65-67). Hfq facilitates base-pairing between complementary sequences of DsrA and *rpoS* which opens the inhibitory stem-loop structure in *rpoS*, which leads to translation. Hfq is believed to be displaced rapidly from its

high-affinity binding site on DsrA through conformational changes in DsrA upon DsrA base-pairing with *rpoS* (68).

Resch *et al.* (2008) demonstrated that the interactions of the *rpoS* 5'-UTR with DsrA not only disrupt the inhibitory secondary structure in the *rpoS* leader but also trigger RNase III cleavage within the intermediate *rpoS*/DsrA duplex (Figure 7). The RNase III cleavage did not significantly affect the stability of the translationally active form of *rpoS* mRNA, which may be attributed to its protection from nucleases by translating ribosomes. RNase III cleavage in the DsrA/*rpoS* duplex apparently prevents recycling of DsrA since also the ncRNA is cleaved (67).

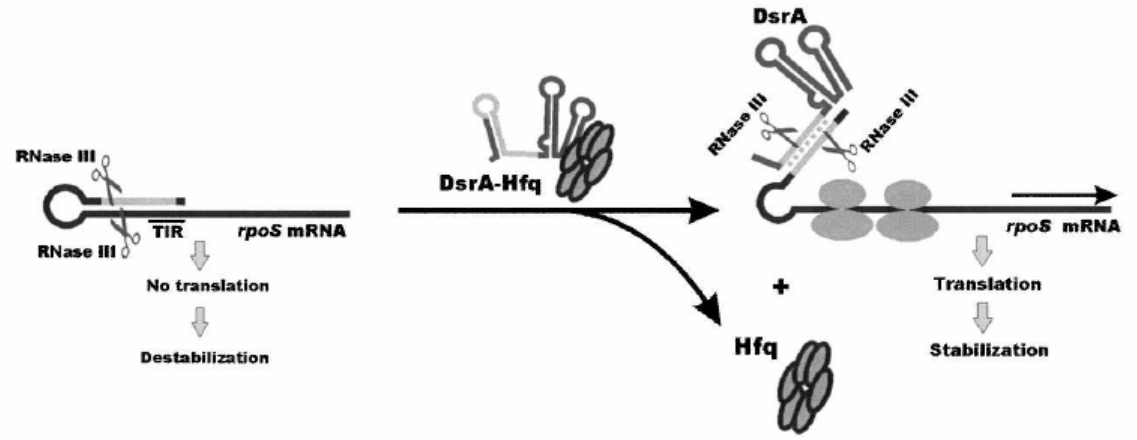

Figure 7. Model for post-transcriptional regulation of *rpoS* expression by RNase III. The translation initiation region (TIR) of the *E. coli rpoS* mRNA is embedded into a complex secondary structure, thereby preventing efficient ribosome binding. RNase III can cleave within the double-stranded segment of this structure, which results in destabilization of the transcript in a wild-type *E. coli* strain when compared to its isogenic counterpart lacking functional RNase III. In contrast to limited synthesis of RpoS under normal growth conditions, the level of RpoS is up-regulated in the presence of increasing amounts of DsrA, which accumulate at low temperature. By base-pairing with the complementary region of the *rpoS* leader, DsrA disrupts the inhibitory secondary structure, thereby facilitating ribosome loading and subsequent translation of RpoS (60). DsrA/*rpoS* duplex formation, which is facilitated by the RNA chaperone Hfq, not only abrogates RNase III cleavage within the *rpoS* leader at positions (−94/−15), but also creates a new RNase III cleavage site within the DsrA/*rpoS* duplex. RNase III cleavage at this site prevents reuse of DsrA for multiple cycles of *rpoS* activation. Moreover, the main body of the DsrA-activated *rpoS* mRNA is covered by translating ribosomes and therefore protected from degradation by ribonucleases (67).

3.8 NMR spectroscopy: flexible amino-acid residues in Hfq

Recently, a NMR analysis on Hfq_{65}, a truncated version of the *E. coli* Hfq protein comprising the first 65 amino acids was performed (Karin Kloiber, unpublished data). ^{15}N NMR relaxation techniques were used that are susceptible to nanosecond-picosecond motion to pinpoint the oligomerization state as well as the local dynamics of ^{15}N-^{1}H bond vectors of the Hfq_{65} protein. ^{15}N longitudinal relaxation (R_1), rotating frame transverse relaxation ($R_{1\rho}$) and $\{^{1}H\}$-^{15}N steady-state NOE experiments were recorded. The relaxation parameters were quite uniform for the majority of the assigned resonances, with average rates amounting to R_1 = 0.39 +/- 0.09 s^{-1}, R_2 = 36.4 +/- 4.0 s^{-1} and a steady state NOE of 0.81 +/- 0.12. The C-terminal residues exhibited typical large-amplitude motions indicated by a very low R_2/R_1 ratio. A "modelfree" analysis (69,70) was performed, revealing that the correlation time of molecular tumbling was 24.5 ns, which is in agreement with a protein of about 45 kD. The analysis of the anisotropy of molecular motion based on the distribution of relaxation parameters required a 3-dimensional model of the molecule. For this purpose the crystal structure of *E. coli* Hfq (pdb entry code 1HK9) (19) was used. The tumbling behaviour could be best characterized using an axially symmetric, oblate structure, which corresponded well with the shape of the hexameric Hfq_{65}: the ratio of rotational diffusion coefficients around the short axis and the long axes of the molecule was determined to be 0.87. Subsequently, the local dynamics of N-H bond vectors was analyzed. The most relevant parameter characterizing bond vector motion is the order parameter S^2, which appears to be very high in all well-ordered regions of Hfq (0.92 +/- 0.047), indicating a very high degree of restriction of motion. (It should be noted that some of the unassigned resonances may pertain to mobile stretches like turn and loop regions). The rigidity inferred from relaxation data is in agreement with the thermal stability of the protein (1). A few residues displayed higher than average dynamics according to the modelfree analysis, most of which are located in the C-terminus (Thr61-Ser65 with low order parameters typical of C-terminal residues) and a short helical region (Lys56-Ser60 which displayed

some degree of flexibility on the ms-µs time-scale and which is implicated in RNA binding). One of the residues outside these regions with noticeable dynamics was Gly29. Like the C-terminus, it displayed large amplitude local motion as inferred from the comparatively small transverse relaxation rate and a slightly increased longitudinal relaxation rate. Fitting the NMR relaxation data of these residues required a model that is characterized by motions on two time-scales (71), often represented by a bond vector moving within a cone superimposed onto the motion of the cone itself. Notably, also residue 28 requires this two-time-scales model. Albeit this is very common for C-terminal stretches of proteins that are often highly mobile, it is less often observed for residues within secondary structure elements. Local motions represent degrees of freedom that often contribute to a macromolecule's ability to interact with other molecules. Gly29 is located in the region connecting β-strands 1 and 2, and is believed to allow for a bend in the 3D structure of Hfq. Its pronounced dynamic properties also indicated a potential function in the accommodation of a ligand.

4 AIM OF THE STUDY

Many *E. coli* Hfq missense mutations were found to be defective in binding ncRNA as well as mRNA which helped to characterize two distinct RNA binding sites located on the homo-hexameric Hfq protein. The proximal site preferably binds ncRNA whereas the distal site binds poly(A) tails (53-56). An NMR spectroscopic analysis suggested Hfq_{Gly29} as a highly flexible amino acid (see 3.8). Hfq_{Gly29}, located on the distal site of the inner ring between β-sheets 1 and 2, is highly conserved among all bacterial Hfq proteins and allows the bending of beta-strand 2 (19). Together with Gly34, Gly29 is a critical residue required for β1 strand curvature, and therefore identical in all Hfq homologues (4). Distal site mutations of amino acids next to Gly29 showed reduced affinity for poly(A) RNA. Changing I30 to D reduced affinity for A_{27} (53) while altering K31 to A had a negative effect on A_{18} binding (54). Hfq_{Y25A} had a lower affinity for rA_7, A_{18} and A_{27} when compared to Hfq_{wt} (53,54,56). Thus, Gly29 was suggested to be involved in RNA binding and therefore essential for function of the RNA chaperone. The aim of this study was to characterize the Hfq missense mutant Hfq_{G29A} with a substitution of glycine 29 for alanine. *In vitro* and *in vivo* methods were applied to address this question.

5 RESULTS

5.1 The *E. coli* strain AM111 *hfq*⁻ (pAHG29A) has reduced levels of RpoS at low temperature

As described in 3.7, the 5'-untranslated region of *rpoS* mRNA forms an inhibitory stem-loop structure, which prevents ribosome binding and translation (59,65). Binding of the ncRNA DsrA to the 5'-UTR of *rpoS* abolishes the secondary structures within the *rpoS* leader and thereby permits translation of *rpoS*. This RNA-RNA interaction is facilitated by Hfq, and especially at low temperatures the action of Hfq is essential (65,66). Therefore, an *hfq*⁻ strain grown at low temperature has very reduced levels of RpoS. Here, I analyzed whether the G29A mutation in *hfq* affects the well established role of Hfq in stimulating *rpoS* translation (Figure 8).

The *E. coli hfq*⁻ AM111 strain carrying a plasmid encoding the Hfq_{wt}, the Hfq_{G29A} mutant and with no *hfq* insert, respectively, were grown at 25 °C, where RpoS expression is strictly dependent on the presence of DsrA and Hfq. Then, a quantitative western-blot analysis was performed to compare the *in vivo* levels of RpoS in the different strains. To determine the relative *in vivo* levels of RpoS, anti-L9 antibodies were used to provide an internal control. The RpoS-specific signals were normalized to the L9-specifc signal and the resulting values were then again normalized to the RpoS signal obtained in the presence of Hfq_{wt} in strain AM111 (pAHfq) (Figure 8B). In addition, a western-blot analysis was carried out with anti-Hfq antibodies to compare the synthesis of Hfq_{wt} and Hfq_{G29A} in strains AM111 (pAHfq) and AM111 (pAHG29A) (Figure 8A). The *hfq*⁻ strain AM111 (pACYC184) (Figure 8, lane 3) showed significantly reduced amounts of RpoS when compared to the hfq_{wt} expressing strain AM111 (pAHfq) (Figure 8, lane 1). AM111 (pAHG29A), the strain expressing the hfq_{G29A} allele (Figure 8, lane 2), had reduced levels of RpoS, comparable to the *hfq*⁻ negative control. These results clearly indicated that Hfq_{G29A} failed to promote DsrA mediated RpoS expression.

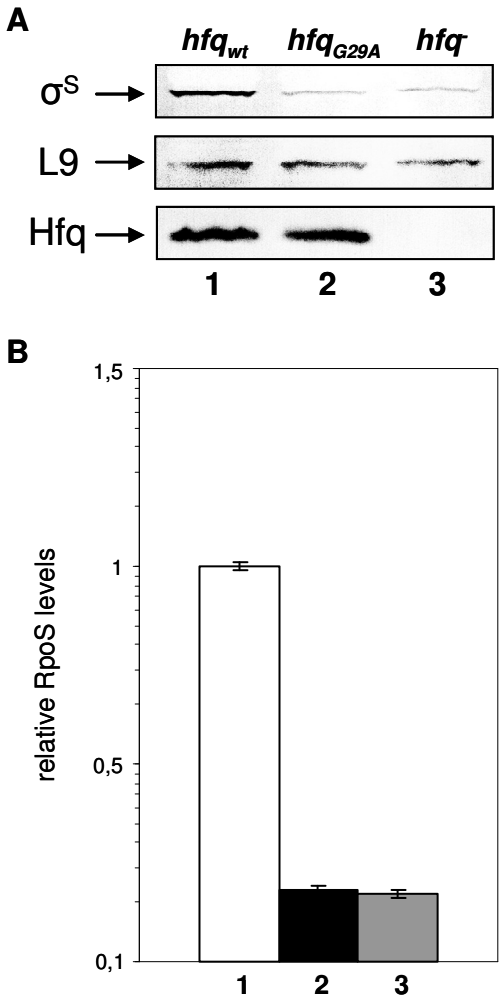

Figure 8. Hfq_{G29A} is defective in mediating DsrA-dependent RpoS expression at low temperatures.
(A) Immunoblot showing σ^S- and Hfq-expression in strain AM111 (pAHfq) (lane 1), in AM111 (pAHG29A) (lane 2) and in AM111 (pACYC184) (lane 3). L9 ribosomal protein served as an internal loading control. Only the relevant sections of the immunoblots showing the σ^S-, L9- and Hfq-specific bands are depicted.
(B) Graphical representation of the σ^S levels in strain AM111 harbouring plasmid pAHfq (white bar; lane 1; Hfq_{wt}), pAHG29A (black bar; lane 2; Hfq_{G29A}) and pACYC184 (grey bar, lane 3; *hfq*$^-$ control) grown at 25 °C in LB medium. Western-blot analysis was carried out with equal amounts of total cellular protein as described in Materials and Methods. Quantification of the western-blot signals was done with ImageQuant software. The values were normalized to the σ^S signals obtained in the presence of Hfq_{wt} in strain AM111 (pAHfq), which was set to 1. The results represent data from three independent experiments. The error bars represent standard deviations.

5.2 Hfq_{G29A} binds RNA with similar affinity as Hfq_{wt}

Since the missense mutation G29A is located on the distal site of the Hfq hexamer it was next tested whether Hfq_{G29A} is defective in RNA binding. Gel mobility shift assays were carried out to analyze the *in vitro* binding behaviour of Hfq_{G29A} towards DsrA and *rpoS* mRNA (Figure 9). 0.05 pmol of 5'-end labelled RNA was incubated with increasing concentrations of Hfq protein and RNA binding of Hfq_{wt} was compared to that of Hfq_{G29A}. As shown in Figure 9A, Hfq_{G29A} is able to bind the ncRNA DsrA with similar affinity as the Hfq_{wt} protein. Gel-shift analysis with DsrA yielded a K_d (= $K_{½}$) of 7 nM for Hfq_{wt} and 8 nM for Hfq_{G29A}.

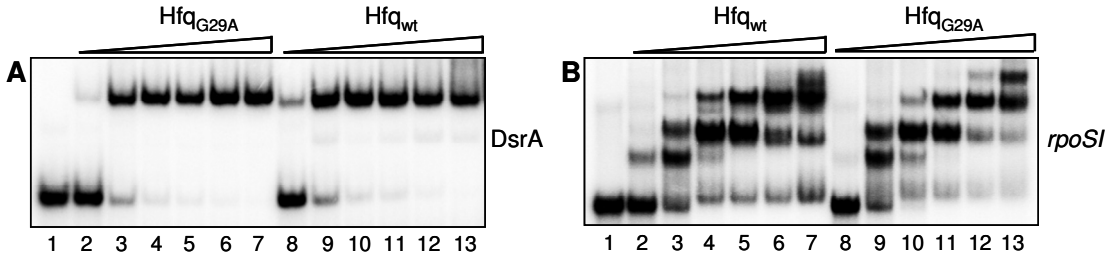

Figure 9. *In vitro* binding of Hfq_{G29A} and Hfq_{wt} to DsrA and *rpoSI* mRNA.
5 nM of 5'-end ^{32}P-labelled DsrA **(A)** and *rpoSI* mRNA **(B)** respectively, was incubated in the absence (lane 1), or in the presence of 5 nM (lanes 2 and 8), 10 nM (lanes 3 and 9), 20 nM (lanes 4 and 10), 40 nM (lanes 5 and 11), 80 nM (lanes 6 and 12) and 160 nM (lanes 7 and 13) Hfq_{G29A}-hexamer or Hfq_{wt}-hexamer.

The gel-shift experiments with *rpoSI* , a truncated version of *rpoS* mRNA comprising nts -146 to +55 (67), showed that the Hfq_{G29A} hexamer did not have any significant binding deficiency when compared to Hfq_{wt} (Figure 9B). The experiment revealed a K_d of ~6 nM for Hfq_{wt} binding to *rpoSI* when compared to 7 nM for Hfq_{G29A}. Thus, altering the glycine at position 29 to alanine did not cause a significant defect in the ability of the hexameric protein to bind ncRNA or mRNA, suggesting that this amino acid residue is not essential for RNA binding of the hexameric Hfq protein.

5.3 Hfq_{G29A} promotes annealing of DsrA and *rpoS in vivo*

As seen from the western-blot assay (Figure 8), the *hfq*$_{G29A}$ strain was defective in RpoS expression at low temperatures. Nevertheless, the gel-shift experiments revealed that the Hfq_{G29A} protein is able to bind to both, DsrA and *rpoSI* (Figure 9). It was therefore conceivable that Hfq_{G29A} is defective in promoting annealing of the two RNAs *in vivo*. Therefore, I made use of an observation made by Resch *et al.* (2008) to test whether Hfq_{G29A} protein affects the annealing of DsrA and *rpoS* mRNA. The translational activation of RpoS expression by the ncRNA DsrA results in an alternative RNase III cleavage at position G_{-112} in the 5'-untranslated region of *rpoS* mRNA (see 3.7). This cleavage occurs upon annealing of DsrA and *rpoS* mRNA and strictly depends on Hfq (Figure 10). Thus, it can serve as a diagnostic marker for DsrA-*rpoS* annealing. The *E. coli* strains JW4130 (pACYC184) (*hfq*$^-$ control), JW4130 (pAHfq); Hfq_{wt} and JW4130 (pAHG29A); Hfq_{G29A} were grown at 25 °C. Total RNA was extracted and primer extension was performed with 5'-end labelled, *rpoS*-specific primer Y39. The separation on a 6% sequencing gel revealed that the RNase III cleavage at position G_{-112} in *rpoS* that was observed in the Hfq_{wt} strain, JW4130 (pAHfq), also occurred in strain JW4130 (pAHG29A), expressing the Hfq_{G29A} mutant protein (Figure 10A, lane 6). In contrast, as expected, RNase III processing did not occur in the *hfq*$^-$ control strain JW4130 (pACYC184) (Figure 10A, lane 7). A western-blot analysis verified that strain JW4130 (pAHG29A) is defective in RpoS synthesis albeit the Hfq_{G29A} protein was present in comparable amounts when compared to strain JW4130 (pAHfq) (Figure 10B).

This result clearly showed that Hfq_{G29A} is able to promote DsrA/*rpoS* annealing despite the significant reduction in the *in vivo* levels of RpoS in strain JW4130 (pAHG29A).

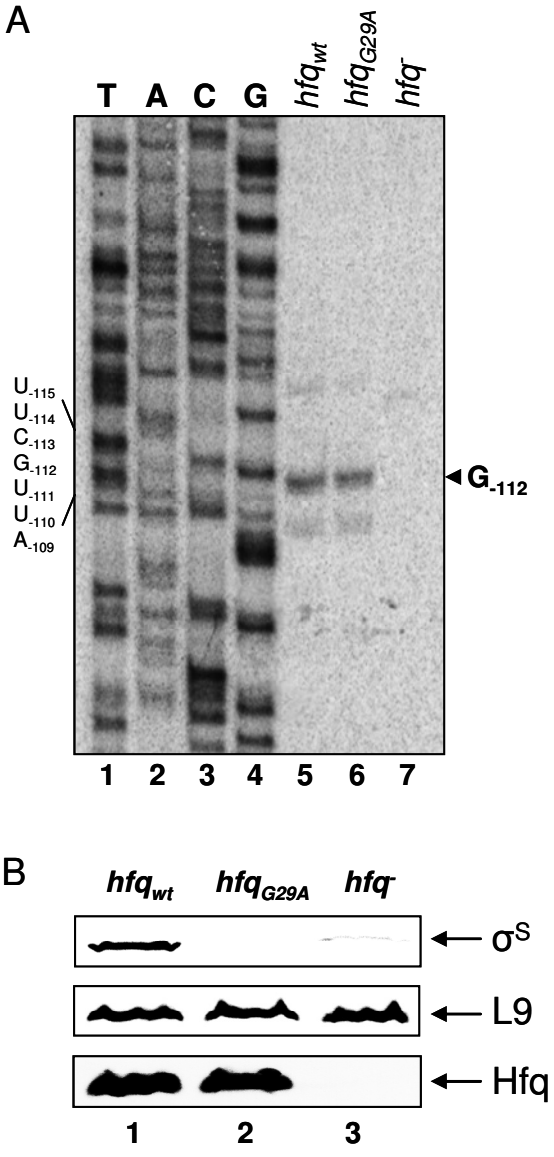

Figure 10. Hfq_{G29A} promotes base pairing between DsrA and *rpoS* mRNA. **(A)** Primer extension analyses of total RNA isolated from strains AM111 (pAHfq) (lane 5), AM111 (pAHG29A) (lane 6) and AM111 (pACYC184) (lane 7), grown at 25 °C in LB medium. The DsrA/Hfq-mediated RNase III cleavage within the 5'-untranslated region of *rpoS* occurs at position G_{-112} (see C). Primer extension products resulting from RNase III cleavage can be detected in strains expressing hfq_{wt} (lane 5) and hfq_{G29A} (lane 6) but not in the hfq^- control (lane 7). **(B)** Determination of Hfq and RpoS levels in strains AM111 (pAHfq) (lane 1), AM111 (pAHG29A) (lane 2) and AM111 (pACYC184) (lane 3) – used for primer extension analysis – by quantitative western-blotting. L9 ribosomal protein served as a loading control. The western-blot analysis was performed as described in Material and Methods. Only the relevant sections of the immunoblots showing the Hfq-, σ^S- and L9-specific bands are depicted. **(C)** The *rpoS*/DsrA complex. The arrows indicate the nucleotide bonds that are cleaved by RNase III. The RNase III cleavage sites G_{-112} in *rpoS* and A_{29} in DsrA were determined by primer extension (67).

5.4 Hfq_{G29A} has an apparent defect in dissociation from DsrA

As shown in Figure 10, Hfq_{G29A}, like Hfq_{wt}, was able to promote annealing between DsrA and the *rpoS* mRNA. However, the quantitative western-blot analysis revealed that the strain expressing *hfq*$_{G29A}$, had strongly decreased levels of RpoS, similar to the *hfq*$^-$ strain (Figure 8). Thus, although Hfq_{G29A} fulfils its role in facilitating annealing between DsrA and *rpoS*, it fails to stimulate *rpoS* translation. As Hfq binds the DsrA-*rpoS* complex fourfold less tightly than DsrA alone, Hfq appears to be rapidly displaced from its high-affinity binding site on DsrA through conformational changes in DsrA which may occur when DsrA base-pairs with *rpoS* mRNA (68). Thus, it was conceivable that the G29A change in Hfq could have a negative effect on displacement of the protein from RNA, which could eventually interfere with translation initiation of *rpoS*.

To address this, ^{32}P-labelled DsrA or *rpoSI* was pre-incubated with a fourfold or eightfold molar excess of hexameric Hfq. Then, unlabelled DsrA or *rpoSI* competitor RNA was added and the RNA-protein complexes were analyzed by electrophoretic mobility shift assay. When compared to Hfq_{wt} (Figure 11A, lanes 2 to 7), DsrA was displaced less rapidly from the Hfq_{G29A} hexamer (Figure 11A, lanes 8 to 13). However, no significant difference was observed when displacement of *rpoSI* from Hfq_{G29A} was compared with that of Hfq_{wt} (Figure 11B).

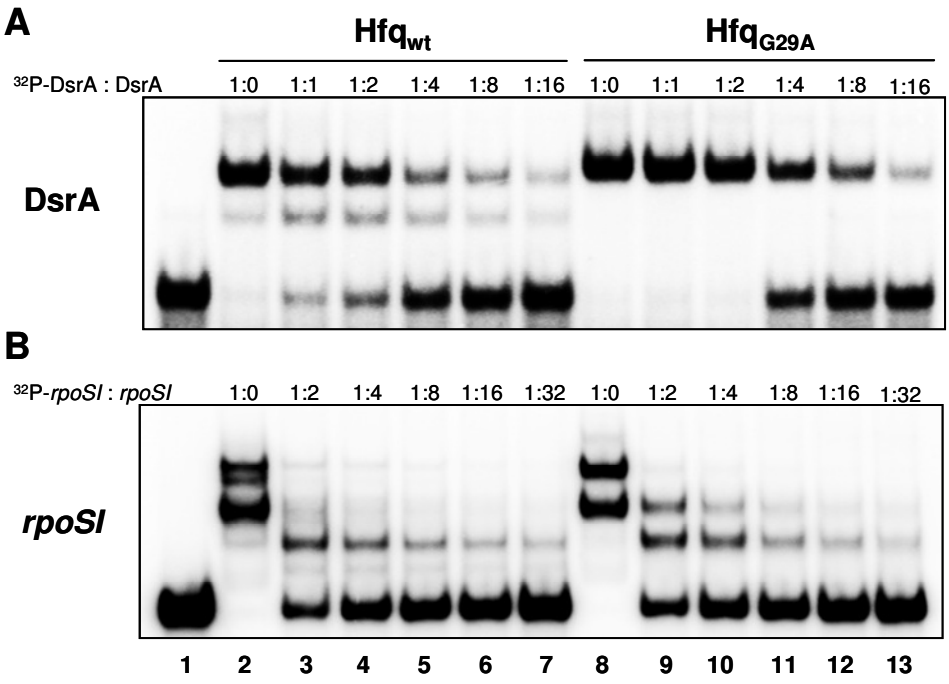

Figure 11. Displacement of DsrA and *rpoSI* from Hfq_{G29A} and Hfq_{wt}.
5′-end ^{32}P-labelled DsrA ncRNA **(A)** and *rpoSI* mRNA **(B)** was incubated in the absence (lane 1), or in the presence of 20 mM (lane 2-13) Hfq_{G29A}-hexamer or Hfq_{wt}-hexamer to form Hfq-RNA complexes. Unlabelled RNA was added as competitor. The molar ratio of labelled RNA to unlabelled competitor RNA is indicated. The molar concentration of either DsrA or *rpoSI* was 5 nM.

6 DISCUSSION

Several Hfq missense mutants with defects in ncRNA or mRNA binding have been reported. However, no mutant Hfq protein has been described that binds DsrA/*rpoS* mRNA and facilitates annealing of the two RNAs, yet fails to mediate activation of *rpoS* translation. Thus, Gly29 may reside in a functional region of Hfq necessary for displacement of the protein from RNA. This hypothesis is corroborated by the impaired release of Hfq_{G29A} from ^{32}P-labelled DsrA in the presence of unlabelled competitor RNA (Figure 11A).

It has previously been described that Hfq possesses ATPase activity (52,56). This finding was surprising, given the small size of Hfq and the seeming lack of homology to proteins with known ATPase motifs. Nevertheless, the N-terminal part of Hfq has homology to the ATP-binding site of the *E. coli* heat-shock protein ClpB (58), which includes the Walker A box. Although the Hfq sequence does not have a canonical Walker A/B ATPase motif, a closer inspection revealed a modified Walker A box (Figure 6) (52). The ClpB Walker A motif, which is highly conserved among other ClpA-like proteins, comprises the sequence **G-X-X-X-X-G-K-T** (X indicates any amino acid) whereas the putative Hfq Walker A box comprises the sequence $\mathbf{G_{29}\text{-}X\text{-}X\text{-}X\text{-}G_{34}\text{-}Q_{35}\text{-}I_{36}}$. Previously, an Hfq_{Q35K} mutant was constructed to obtain a canonical Walker A box motif. The kinetic parameters of the Hfq_{Q35K} mutant in binding and hydrolyzing ATP were similar to those of the wild-type Hfq (52). Arluison *et al.* (2007) modelled the location of the ATP binding site within Hfq and analyzed the effect of ATP on Hfq-RNA complexes (56). The key amino acids forming the putative ATP-binding cleft (Tyr25 and Gln52) are highly conserved in the bacterial Hfq proteins; and Lys31, located within the modified Walker A box of Hfq, is moderately conserved. An amino acid change of Tyr25 to alanine, which is in close vicinity of Gly29, results in reduced ATP binding and reduced ATPase activity of the Hfq_{Y25A} (56).

In addition, electron microscopic data indicated that binding of both, RNA and ATP, is accompanied by a detectable distortion in the Hfq sixfold symmetry. The

results of RNA footprinting and binding analyses suggested that ATP binding by the Hfq–RNA complex results in its significant destabilization (56).

Recently, the 3D-structure of Hfq_{65} in complex with dAMP was solved at 1.8 Å resolution (Mads Beich-Frandsen, unpublished results). The substrate used to form the complex with Hfq_{65} was dADP but was apparently hydrolyzed to dAMP in the buffer. The adenine portion of dAMP is bound between Tyr25 and Ile31 on the distal site of the hexamer via aromatic stacking (Figure 12). The phosphoester tail protrudes away from the Hfq hexamer and the hydroxyl groups of the sugar are in hydrogen bonding distance to the carbonyl group of Gly29. This is at variance with the model published by Arluison *et al.* (2007), where the triphosphate portion of the ATP molecule was reported to point to the outer rim, at the "L4" face of the hexameric Hfq molecule (56).

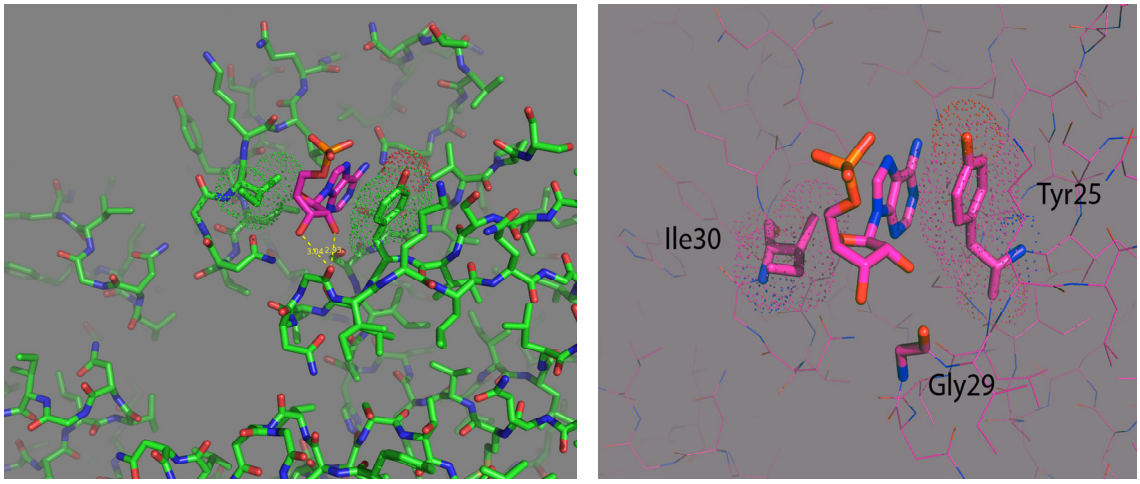

Figure 12. Crystal Structure of *E. coli* Hfq_{65} in complex with dAMP. View on the distal site of the Hfq hexamer. The adenine portion of dAMP is bound between Ile30 and Tyr25 via aromatic stacking. The hydroxyl groups of the sugar are in hydrogen bonding distance to the carbonyl group of Gly29 (indicated by dotted lines). The carbon atoms of dAMP are shown in pink, phosphor in orange, oxygen in red and nitrogen in blue (Mads Beich-Frandsen, unpublished data).

Taking into account that the glycine 29 is highly conserved in other bacterial Hfq proteins, and that it is part of the modified Walker A motif in Hfq, which is thought to be involved in ATP binding, the G29A mutation may negatively affect the ability of Hfq to bind ATP. This could explain the negative effect on displacement of RNA from the mutant Hfq_{G29A} protein. Moreover, this

hypothesis would rationalize why Hfq_{G29A} is still able to bind and stimulate annealing of DsrA and *rpoS*. However, after RNase III processing, the Hfq_{G29A} may not be displaced because no ATP can be bound by Hfq_{G29A}, which in turn could interfere with translation initiation complex function on *rpoS* mRNA.

7 MATERIALS AND METHODS

7.1 Bacterial strains and plasmids

All *E. coli* strains were grown in Luria-Bertani (LB) broth (72) at 37 °C or 25 °C supplemented with appropriate antibiotics to maintain the respective plasmids. Final concentrations of 100 µg/ml ampicillin, 20 µg/ml kanamycin and 20 µg/ml chloramphenicol were used. If glucose was added to cultures, the final concentration was 1%. The bacterial strains and plasmids used in this study are listed in Table 1.

Table 1. Bacterial strains and plasmids used in this study.

***E.coli* Strain**	**Genotype**	**Source/Reference**
TOP10	*F¯ mcrAΔ(mrr-hsdRMS-mcrBC) φ80lacX74 nupG recA1 araD139 Δ(ara-leu)7697 galE15 galK16 rpsL(Str^R)*	Invitrogen
TOP10F'	*TOP10 with lacI^q*	Invitrogen
MC4100	*F¯ araD139 Δ(argF-lac)U169 rspL150 relA1 flbB5301 fruA25 deoC1 ptsF25 e14-*	(73)
AM111	*MC4100 hfq::Ω*	(74)
AM111F'	*AM111 with lacI^q*	(75)
BW25113	*rrnB3 ΔlacZ4787 hsdR514 Δ(araBAD)567 Δ(rhaBAD)568 rph-1*	(76)
JW4130	*BW25113 hfq::Ω*	(76)

Plasmid	Genotype	Source/Reference
pUC19	*Amp^R, lacZ` mit MCS*	New England Biolabs
pUH5	*pUC19 encoding Hfq$_{wt}$ protein*	(77)
pUHG29A	*pUC19 encoding Hfq$_{G29A}$ protein*	this study
pACYC184	*cat (Cm^R), Tc^R, p15A-ori*	Fermentas
pAHfq	*pACYC184 encoding Hfq$_{wt}$ protein; Tc^R*	(57)
pAHG29A	*pACYC184 encoding Hfq$_{G29A}$ protein; Tc^R*	this study

7.2 Construction of plasmid pUHG29A

To construct the *hfq$_{G29A}$* allele the *hfq* forward primer C19 (5'-GCTCTAGAAATATAATAGTTTAACTTTAAGAAGGAGATATACATATGGCTAAGGGGCAATCTTTACAAGATCCGTTCCT-3'), containing a *Xba*I site, and the *hfq* specific T45 primer (5'-AGACTCGATTTGCCCTTGCAGCTTAATAGCATTCACCAAA-3') were used together with the template plasmid pUH5 in a PCR reaction (see below). The PCR product was then used with the *hfq* reverse primer B19 (5'-GGAATTCCCGTGTAAAAAAACAGCCCGAAAC-3'), containing an *EcoR*I site, in another PCR reaction with pUH5 to amplify the *hfq$_{G29A}$* allele. The PCR product comprising the *hfq$_{G29A}$* allele was cleaved with restriction enzymes *EcoRI* (from B19) and *XbaI* (from C19) and cloned into the *EcoR*I and *Xba*I sites of plasmid pUC19, resulting in plasmid pUHG29A. The plasmid carries the pMB1 replicon (ColE1) and the *bla* gene (conferring ampicillin-resistance) from pUC19; the *hfq$_{G29A}$* allele is under P_{lacPO} control. The primers used to construct plasmid pUHG29A are listed in Table 2.

PCR-program:

Hot Start	1x	5min.	94°C
	30x	30sec. 40sec. 30sec.	94°C 55°C 68°C

Table 2. Oligonucleotides used for cloning.

Primer /Name	**Sequence**	**Properties**
C19	5′- GC**TCTAGA**AATATAATAGTTTAACTTTAA GAAGGAGATATACATATGGCTAAGGGGCA ATCTTTACAAGATCCGTTCCT-3′	*hfq* forward primer *Xba*I cleavage site marked bold
B19	5′- G**GAATTC**CCGTGTAAAAAAACAGCCCGA AAC-3′	*hfq* reverse primer *EcoR*I cleavage site marked bold
T45	5′- AGACTCGATTTGCCCTTGCAGCTTAAT**AG C**ATTCACCAAA-3′	reverse primer for hfq_{G29A} triplet changed to alanine marked bold

7.3 Construction of plasmid pAHG29A

The hfq_{G29A} gene, together with the *lac* operon containing CAP protein binding site, the *lac* promoter and the *lac* repressor binding site (derived from pUC19), was obtained from plasmid pUHG29A after cleavage with *Pvu*II. The allele was then cloned into plasmid pACYC184 (cleaved with *Nru*I and *EcoR*V) to produce plasmid pAHG29A. The cleavage of plasmid pACYC184 with *Nru*I and *EcoR*V destroyed the *tet* gene (Tc^R), encoding tetracycline resistance. Therefore plasmid pAHG29A contains only one resistance gene (*cat*, Cm^R) when compared to the parental plasmid pACYC184.

7.4 Purification of protein Hfq_{G29A} and Hfq_{wt}

Hfq_{G29A} was purified using the His-tag technology. Since Hfq contains a natural His-tag it binds to the Ni-agarose resin (Mads Beich-Frandsen, personal communication). *E. coli* strains AM111F' containing plasmid pUHG29A (encoding the hfq_{G29A} gene) and pUH5 (encoding the hfq_{wt} gene) were grown in LB medium supplemented with ampicillin (100 µg/ml) and kanamycin (20 µg/ml). Expression of hfq_{G29A} and hfq_{wt} was induced at an OD_{600} of 0.8 by addition of isopropyl-β-D-thiogalactopyranoside (IPTG) to a final concentration of 1 mM. After 2 h of further growth, the cells were collected by centrifugation (5000 rpm; 4 °C) and resuspended in lysis buffer (50 mM Tris pH 8, 1.5 M NaCl, 250 mM $MgCl_2$, 5 mM DTT, 1 mM PMSF) lacking PMSF and DTT (1 ml per 25 ml cell culture) to wash the cells. Upon centrifugation, the pellets were stored at -20 °C. Two pellets from 25 ml cell culture were resuspended in 1 ml ice-cold lysis buffer and the cells were lysed by sonication. After addition of DNAse I (10 µg/ml) and incubation on ice for 20 min, the cell debris was pelleted by centrifugation at 14.000 rpm (4 °C; 20 min). The supernatant was transferred into new 2 ml tubes and heated for 20 min at 85 °C to denature mesophilic proteins. The denatured proteins were subsequently removed by centrifugation at 18.000 rpm and 4 °C for 20 min. The supernatant was loaded on a column, containing 1 ml Ni-NTA Agarose (The Ni-NTA agarose was pre-washed with 10 ml lysis buffer lacking PMSF and DTT). The protein bound to the Ni-NTA agarose was washed 7 times with 10 ml washing buffer (50mM Tris pH 8, 200 mM NaCl, 3 M Urea), and then 3 times with 10 ml GF buffer (50mM Tris pH 8, 200 mM NaCl) to remove Urea. Finally, the bound protein was eluted by increasing concentrations of imidazole in GF buffer:

1. fraction: 400 µl 0.1 M Imidazole
2. fraction: 400 µl 0.25 M Imidazole
3. fraction: 400 µl 0.5 M Imidazole
4. fraction: 400 µl 0.5 M Imidazole
5. fraction: 400 µl 0.5 M Imidazole.

The fractions were then analyzed on a 12% polyacrylamide (PAA) protein gel using Coomassie blue staining to determine the fractions with the highest concentration of protein. The fractions were dialyzed using benzoylated dialysis tubings (Sigma). The protein fractions were dialysed overnight at 4 °C in 1 L GF buffer:ddH_2O 1:1 and again analyzed on a 12% PAA protein gel using Coomassie blue staining. The protein concentration was determined using the BCA^{TM} Protein Assay kit (Thermo Scientific).

7.5 Western-blot analysis

The *E. coli* strain AM111 harbouring plasmids pACYC184 (*hfq*$^-$ control), pAHfq (encoding *hfq*$_{wt}$) and pAHG29A (encoding *hfq*$_{G29A}$) were used to determine the levels of RpoS (σ^S) by quantitative immunoblotting. The cells were grown at 25 °C in LB medium containing the appropriate antibiotics. Samples were withdrawn at an OD_{600} of 0.7 and boiled in 1x Laemmli-buffer. Equal amounts of total cellular extracts were then electrophoretically separated on 12% SDS-polyacrylamide gels and electroblotted to a nitrocellulose membrane. The blot was blocked with 5% dry milk in TBS buffer and then probed with anti-σ^S antibody (NeoClone) and anti-L9 antibody, detecting the ribosomal protein L9 (internal loading control). To confirm expression of Hfq_{wt} and Hfq_{G29A} in the respective strains, a second western-blot was carried out, using an anti-Hfq antibody (78). The antibody-antigen complexes were visualized with alkaline phosphatase-conjugated antibodies (78). The quantification of the RpoS-specific bands was performed with ImageQuant software.

7.6 Gel-shift assays

Hfq_{wt} and Hfq_{G29A} proteins were purified from AM111F' (pUHG29A) and AM111F' (pUH5) cells as described above. The RNAs used in the gel-shift assays were 5'-end labelled using [γ-^{32}P]-ATP (Amersham Pharmacia Biotech). The RNAs (5 nM) were incubated without or with increasing amounts of purified Hfq-hexamer protein (as indicated in the legend to Figure 9) in a 10 µl reaction in binding buffer (10 mM Tris pH 7.4, 60 mM NH_4Cl, 6 mM β-mercaptoethanol, 2 mM MgOAc, 10ng/µl yeast tRNA) for 5 min at room temperature. After cooling on ice and addition of 40% glycerol to a final concentration of 10%, the samples were loaded on a non-denaturing 5% polyacrylamide gel. The electrophoresis was performed in TAE buffer at 100-130 V for 3-5 h and the radioactive bands were visualized using a PhosphoImager (Molecular Dynamics). *rpoSI*, a shortened version of *rpoS* mRNA (nts -146 to +55), comprising a part of the 5'-UTR containing the Hfq- and DsrA-binding sites, has been previously described (67).

7.7 Primer extension analysis

E. coli strains JW4130 (pACYC184), JW4130 (pAHfq) and JW4130 (pAHG29A) were grown at 25 °C to an OD_{600} of 0.6 in LB medium containing the appropriate antibiotics. Then, the cells were harvested and total RNA was purified by the hot phenol method (79).

In addition, aliquots were withdrawn and Hfq and RpoS synthesis was determined by western-blot analysis as described above. Primer extension analysis was performed using aliquots of 30 µg of total RNA as previously described (80). 5'-[^{32}P]-labelled *rpoS*-specific primer Y39 (5'-TCCGTTCTCATCAAATTCCGCATC-3') was annealed to RNA and cDNA synthesis was performed for 60 min at 45 °C. The resulting product was mixed 1:1 with MMLV loading dye and separated on a 6% sequencing gel together with a sequencing ladder using oligonucleotide Y39 and *in vitro* transcribed $rpoS_{652}$

(57). Finally, the cleavage products were visualized using a PhosphoImager (Molecular Dynamics).

7.8 Competition bandshift assays

Hfq_{wt} and Hfq_{G29A} proteins were purified from strains AM111F' (pUHG29A) and AM111F' (pUH5) as described above. DsrA and *rpoSI* (67) were 5'-end labelled with [γ-^{32}P]-ATP (Amersham Pharmacia Biotech). Labelled RNA (5 nM) was pre-incubated without or with a fourfold (DsrA) or eightfold (*rpoSI*) molar excess of hexameric Hfq for 10 min at room temperature in binding buffer (10 mM Tris pH 7.4, 60 mM NH_4Cl, 6 mM β-mercaptoethanol, 2 mM MgOAc, 10 ng/µl yeast tRNA) and then cooled on ice. Increasing amounts of unlabelled competitor RNA (as described in the legend to Figure 11) were added and incubation was continued at room temperature for 10 min. After cooling on ice and addition of 40% glycerol to a final concentration of 10%, the samples were loaded on a non-denaturing 4% polyacrylamide gel. Electrophoresis was performed in TAE buffer at 100-130V for 3-5 h and the radioactive bands were visualized using a PhosphoImager (Molecular Dynamics).

8 APPENDIX

8.1 Buffers / Solutions

30% PAA stock solution (29:1):

290 g	Acrylamide
10 g	N-N-methylenbisacrylamide
add to 1 L	$_{dd}H_2O$

40% PAA stock solution (38:2):

380 g	Acrylamide
20 g	N-N-methylenbisacrylamide
add to 1 L	$_{dd}H_2O$

DNA-Gel:

TBE (10x):

per litre	
108 g	Tris
55 g	Boric Acid
100 ml	0.5 M EDTA, pH 8

6% PAA solution:

30 ml	40% (38:2) PAA
20 ml	10x TBE
150 ml	$_{dd}H_2O$

6% PAA gel (DNA):

5 ml	6% PAA
70 µl	10% APS
7 µl	TEMED

0.8% Agarose gel:

2,4 g	Agarose in 300 ml 0.5x TBE

DNA loading dye:

10 mM	Tris, pH 7.6
0.15%	Orange G
0.03%	Xylene Cyanol FF
60%	Glycerol
60 mM	EDTA

DNA elution buffer:

0.3 M	NaCl
3 mM	EDTA
30 mM	Tris, pH 7.6

Protein-Gels:

10x SDS-Page running buffer:

per litre	
30 g	Tris
144 g	Glycine
10 g	SDS

30% PAA stock solution (29:1):

290 g	Acrylamide
10 g	N-N-methylenbisacrylamide
add to 1 L	$_{dd}H_2O$

40% PAA stock solution (38:2):

380 g	Acrylamide
20 g	N-N-methylenbisacrylamide
add to 1 L	$_{dd}H_2O$

Protein PAA gel (12%):

	Separative gel (12%)
1.4 ml	$_{dd}H_2O$
1 ml	Lower-Tris
1.6 ml	30% PAA
14.4 µl	10% APS
7.2 µl	TEMED
	Collecting gel
1.4 ml	$_{dd}H_2O$
0.6 ml	Upper-Tris
0.4 ml	30% PAA
10 µl	10% APS
20 µl	TEMED

1x Laemmli Buffer:

50 mM	Tris, pH 6.8
2%	SDS
10%	Glycerol
0.1%	Bromphenol Blue
1%	B-Mercaptoethanol

2x Laemmli Buffer:

100 mM	Tris, pH 6.8
4%	SDS
20%	Glycerol
0.2%	Bromphenol Blue
2%	B-Mercaptoethanol

Coomassie staining solution:

45%	Methanol
10%	Acetic Acid
0.25%	Coomassie Blue
	in $_{dd}H_2O$

De-stain solution:

45%	Methanol
10%	Acetic Acid
	in $_{dd}H_2O$

<u>Western Blot:</u>

TBS (10x):

per litre	
80 g	NaCl
2 g	KCl
250 ml	1 M Tris, pH 7,5

Antibody-solution:

antibody	1:10000 dilution in 1xTBS
per 25 ml	
0.3 g	BSA
50 µl	10% NaN_3
add to 25 ml	1xTBS
2.5 µl	antibody

Transfer Buffer:

per litre	
2,9 g	Glycine
5,8 g	Tris
	adjust to pH 8.3 with HCl
0,37 g	SDS
200 ml	Methanol

Alkaline phosphatase buffer:

100 mM	NaCl
5 mM	MgCl2
100 mM	Tris, pH 9.5

BCIP-solution:

0.5 g	BCIP
10 ml	Dimethylformamid (100%)

NBT-solution:

0.5 g	NBT
10 ml	Dimethylformamid (70%)

Protein Purification:

Lysis buffer:

50 mM	Tris, pH 8
1.5 M	NaCl
250 mM	$MgCl_2$
5 mM	DTT (fresh into warm buffer)
1 mM	PMSF (fresh into warm buffer)

GF buffer:

50 mM	Tris, pH 8
200 mM	NaCl

Washing buffer:

50 mM	Tris, pH 8
200 mM	NaCl
3 M	Urea

Bandshift Assays:

non-denaturing 4% PAA Gel:

50 mM	40% PAA
0,8 ml	50x TAE
add to 40 ml	$_{dd}H_20$
250 µl	10% APS
50 µl	TEMED

50x TAE:

per liter	
242 g	Tris
100 ml	0,5M EDTA (pH 8)
57,1 ml	Acetic Acid (glacial)
add to 1 L	$_{dd}H_2O$ (final pH 8)

5xVD$^+$ Buffer:

50 mM	Tris, pH 7,4
300 mM	NH_4Cl
30 mM	B-Mercaptoethanol
2 mM	MgOAc

Primer Extension:

8% sequencing gel:

24 g	Urea
7,5 ml	40% PAA
5 ml	10x TBE
add to 50 ml	$_{dd}H_2O$
250 µl	10% APS
25 µl	TEMED

10x RT$^-$ Buffer:

0,5 M	Tris, pH 8,3
0,6 M	NaCl
0,1 M	DTT
	in DEPC-H_2O

10x RT$^+$ Buffer:

0,5 M	Tris, pH 8,3
0,6 M	NaCl
0,1 M	DTT
0,02 M	$MgCl_2$
	in DEPC-H_2O

5x dNTPs:

6 µl	100 mM dNTPs
16 µl	10x RT$^+$ Buffer
DEPC-H_2O	120 µl

9 REFERENCES

1. Franze de Fernandez, M.T., Eoyang, L. and August, J.T. (1968) Factor fraction required for the synthesis of bacteriophage Qbeta-RNA. *Nature*, **219**, 588-590.
2. Miranda, G., Schuppli, D., Barrera, I., Hausherr, C., Sogo, J.M. and Weber, H. (1997) Recognition of bacteriophage Qbeta plus strand RNA as a template by Qbeta replicase: role of RNA interactions mediated by ribosomal proteins S1 and host factor. *Journal of Molecular Biology*, **267**, 1089-1103.
3. Tsui, H.C., Leung, H.C. and Winkler, M.E. (1994) Characterization of broadly pleiotropic phenotypes caused by an *hfq* insertion mutation in *Escherichia coli* K-12. *Molecular Microbiology*, **13**, 35-49.
4. Sun, X., Zhulin, I. and Wartell, R.M. (2002) Predicted structure and phyletic distribution of the RNA-binding protein Hfq. *Nucleic Acids Research*, **30**, 3662-3671.
5. Kajitani, M., Kato, A., Wada, A., Inokuchi, Y. and Ishihama, A. (1994) Regulation of the *Escherichia coli hfq* gene encoding the host factor for phage Q beta. *Journal of Bacteriology*, **176**, 531-534.
6. Vytvytska, O., Jakobsen, J.S., Balcunaite, G., Andersen, J.S., Baccarini, M. and von Gabain, A. (1998) Host factor I, Hfq, binds to *Escherichia coli ompA* mRNA in a growth rate-dependent fashion and regulates its stability. *Proceedings of the National Academy of Sciences of the United States of America*, **95**, 14118-14123.
7. Tsui, H.C., Feng, G. and Winkler, M.E. (1997) Negative regulation of *mutS* and *mutH* repair gene expression by the Hfq and RpoS global regulators of *Escherichia coli* K-12. *Journal of Bacteriology*, **179**, 7476-7487.
8. Sledjeski, D.D., Whitman, C. and Zhang, A. (2001) Hfq is necessary for regulation by the untranslated RNA DsrA. *Journal of Bacteriology*, **183**, 1997-2005.
9. Zhang, A., Wassarman, K.M., Ortega, J., Steven, A.C. and Storz, G. (2002) The Sm-like Hfq protein increases OxyS RNA interaction with target mRNAs. *Mol Cell*, **9**, 11-22.
10. Geissmann, T.A. and Touati, D. (2004) Hfq, a new chaperoning role: binding to messenger RNA determines access for small RNA regulator. *The EMBO Journal*, **23**, 396-405.
11. Updegrove, T., Wilf, N., Sun, X. and Wartell, R.M. (2008) Effect of Hfq on RprA-*rpoS* mRNA pairing: Hfq-RNA binding and the influence of the 5' *rpoS* mRNA leader region. *Biochemistry*, **47**, 11184-11195.
12. Zhang, A., Wassarman, K.M., Rosenow, C., Tjaden, B.C., Storz, G. and Gottesman, S. (2003) Global analysis of small RNA and mRNA targets of Hfq. *Molecular Microbiology*, **50**, 1111-1124.
13. Argaman, L., Hershberg, R., Vogel, J., Bejerano, G., Wagner, E.G., Margalit, H. and Altuvia, S. (2001) Novel small RNA-encoding genes in the intergenic regions of *Escherichia coli*. *Curr Biol*, **11**, 941-950.
14. Valentin-Hansen, P., Eriksen, M. and Udesen, C. (2004) The bacterial Sm-like protein Hfq: a key player in RNA transactions. *Molecular Microbiology*, **51**, 1525-1533.

15. Moller, T., Franch, T., Hojrup, P., Keene, D.R., Bachinger, H.P., Brennan, R.G. and Valentin-Hansen, P. (2002) Hfq: a bacterial Sm-like protein that mediates RNA-RNA interaction. *Mol Cell*, **9**, 23-30.
16. Schumacher, M.A., Pearson, R.F., Moller, T., Valentin-Hansen, P. and Brennan, R.G. (2002) Structures of the pleiotropic translational regulator Hfq and an Hfq-RNA complex: a bacterial Sm-like protein. *The EMBO Journal*, **21**, 3546-3556.
17. Azam, T.A. and Ishihama, A. (1999) Twelve species of the nucleoid-associated protein from *Escherichia coli*. Sequence recognition specificity and DNA binding affinity. *J Biol Chem*, **274**, 33105-33113.
18. Brennan, R.G. and Link, T.M. (2007) Hfq structure, function and ligand binding. *Current Opinion in Microbiology*, **10**, 125-133.
19. Sauter, C., Basquin, J. and Suck, D. (2003) Sm-like proteins in Eubacteria: the crystal structure of the Hfq protein from *Escherichia coli*. *Nucleic Acids Research*, **31**, 4091-4098.
20. Carmichael, G.G., Weber, K., Niveleau, A. and Wahba, A.J. (1975) The host factor required for RNA phage Qbeta RNA replication *in vitro*. Intracellular location, quantitation, and purification by polyadenylate-cellulose chromatography. *J Biol Chem*, **250**, 3607-3612.
21. Nikulin, A., Stolboushkina, E., Perederina, A., Vassilieva, I., Bläsi, U., Moll, I., Kachalova, G., Yokoyama, S., Vassylyev, D., Garber, M. *et al.* (2005) Structure of *Pseudomonas aeruginosa* Hfq protein. *Acta Crystallogr D Biol Crystallogr*, **61**, 141-146.
22. Arluison, V., Derreumaux, P., Allemand, F., Folichon, M., Hajnsdorf, E. and Regnier, P. (2002) Structural Modelling of the Sm-like Protein Hfq from *Escherichia coli*. *Journal of Molecular Biology*, **320**, 705-712.
23. Toro, I., Basquin, J., Teo-Dreher, H. and Suck, D. (2002) Archaeal Sm proteins form heptameric and hexameric complexes: crystal structures of the Sm1 and Sm2 proteins from the hyperthermophile *Archaeoglobus fulgidus*. *Journal of Molecular Biology*, **320**, 129-142.
24. Achsel, T., Brahms, H., Kastner, B., Bachi, A., Wilm, M. and Luhrmann, R. (1999) A doughnut-shaped heteromer of human Sm-like proteins binds to the 3'-end of U6 snRNA, thereby facilitating U4/U6 duplex formation *in vitro*. *The EMBO Journal*, **18**, 5789-5802.
25. Achsel, T., Stark, H. and Lührmann, R. (2001) The Sm domain is an ancient RNA-binding motif with oligo(U) specificity. *Proceedings of the National Academy of Sciences of the United States of America*, **98**, 3685-3689.
26. Collins, B.M., Harrop, S.J., Kornfeld, G.D., Dawes, I.W., Curmi, P.M. and Mabbutt, B.C. (2001) Crystal structure of a heptameric Sm-like protein complex from archaea: implications for the structure and evolution of snRNPs. *Journal of Molecular Biology*, **309**, 915-923.
27. Toro, I., Thore, S., Mayer, C., Basquin, J., Seraphin, B. and Suck, D. (2001) RNA binding in an Sm core domain: X-ray structure and functional analysis of an archaeal Sm protein complex. *The EMBO Journal*, **20**, 2293-2303.
28. He, W. and Parker, R. (2000) Functions of Lsm proteins in mRNA degradation and splicing. *Curr Opin Cell Biol*, **12**, 346-350.
29. Bouveret, E., Rigaut, G., Shevchenko, A., Wilm, M. and Seraphin, B. (2000) A Sm-like protein complex that participates in mRNA degradation. *The EMBO Journal*, **19**, 1661-1671.

30. Hermann, H., Fabrizio, P., Raker, V.A., Foulaki, K., Hornig, H., Brahms, H. and Lührmann, R. (1995) snRNP Sm proteins share two evolutionarily conserved sequence motifs which are involved in Sm protein-protein interactions. *The EMBO Journal*, **14**, 2076-2088.
31. Seraphin, B. (1995) Sm and Sm-like proteins belong to a large family: identification of proteins of the U6 as well as the U1, U2, U4 and U5 snRNPs. *The EMBO Journal*, **14**, 2089-2098.
32. de Haseth, P.L. and Uhlenbeck, O.C. (1980) Interaction of *Escherichia coli* host factor protein with oligoriboadenylates. *Biochemistry*, **19**, 6138-6146.
33. de Haseth, P.L. and Uhlenbeck, O.C. (1980) Interaction of *Escherichia coli* host factor protein with Q beta ribonucleic acid. *Biochemistry*, **19**, 6146-6151.
34. Brescia, C.C., Mikulecky, P.J., Feig, A.L. and Sledjeski, D.D. (2003) Identification of the Hfq-binding site on DsrA RNA: Hfq binds without altering DsrA secondary structure. *RNA*, **9**, 33-43.
35. Moll, I., Leitsch, D., Steinhauser, T. and Bläsi, U. (2003) RNA chaperone activity of the Sm-like Hfq protein. *EMBO Rep*, **4**, 284-289.
36. Vecerek, B., Moll, I. and Bläsi, U. (2005) Translational autocontrol of the *Escherichia coli hfq* RNA chaperone gene. *RNA*, **11**, 976-984.
37. Kawamoto, H., Koide, Y., Morita, T. and Aiba, H. (2006) Base-pairing requirement for RNA silencing by a bacterial small RNA and acceleration of duplex formation by Hfq. *Molecular Microbiology*, **61**, 1013-1022.
38. Masse, E. and Gottesman, S. (2002) A small RNA regulates the expression of genes involved in iron metabolism in *Escherichia coli*. *Proceedings of the National Academy of Sciences of the United States of America*, **99**, 4620-4625.
39. Vecerek, B., Moll, I. and Bläsi, U. (2007) Control of Fur synthesis by the non-coding RNA RyhB and iron-responsive decoding. *The EMBO Journal*, **26**, 965-975.
40. Vytvytska, O., Moll, I., Kaberdin, V.R., von Gabain, A. and Bläsi, U. (2000) Hfq (HF1) stimulates *ompA* mRNA decay by interfering with ribosome binding. *Genes & Development*, **14**, 1109-1118.
41. Folichon, M., Arluison, V., Pellegrini, O., Huntzinger, E., Regnier, P. and Hajnsdorf, E. (2003) The poly(A) binding protein Hfq protects RNA from RNase E and exoribonucleolytic degradation. *Nucleic Acids Research*, **31**, 7302-7310.
42. Masse, E., Escorcia, F.E. and Gottesman, S. (2003) Coupled degradation of a small regulatory RNA and its mRNA targets in *Escherichia coli*. *Genes & Development*, **17**, 2374-2383.
43. Moll, I., Afonyushkin, T., Vytvytska, O., Kaberdin, V.R. and Bläsi, U. (2003) Coincident Hfq binding and RNase E cleavage sites on mRNA and small regulatory RNAs. *RNA*, **9**, 1308-1314.
44. Afonyushkin, T., Vecerek, B., Moll, I., Bläsi, U. and Kaberdin, V.R. (2005) Both RNase E and RNase III control the stability of *sodB* mRNA upon translational inhibition by the small regulatory RNA RyhB. *Nucleic Acids Research*, **33**, 1678-1689.
45. Mackie, G.A. (1991) Specific endonucleolytic cleavage of the mRNA for ribosomal protein S20 of *Escherichia coli* requires the product of the *ams* gene *in vivo* and *in vitro*. *Journal of Bacteriology*, **173**, 2488-2497.

46. Mackie, G.A. and Genereaux, J.L. (1993) The role of RNA structure in determining RNase E-dependent cleavage sites in the mRNA for ribosomal protein S20 *in vitro*. *Journal of Molecular Biology*, **234**, 998-1012.
47. McDowall, K.J., Lin-Chao, S. and Cohen, S.N. (1994) A+U content rather than a particular nucleotide order determines the specificity of RNase E cleavage. *J Biol Chem*, **269**, 10790-10796.
48. Herschlag, D. (1995) RNA chaperones and the RNA folding problem. *The Journal of Biological Chemistry*, **270**, 20871-20874.
49. Tsuchihashi, Z. and Brown, P.O. (1994) DNA strand exchange and selective DNA annealing promoted by the human immunodeficiency virus type 1 nucleocapsid protein. *J Virol*, **68**, 5863-5870.
50. Clodi, E., Semrad, K. and Schroeder, R. (1999) Assaying RNA chaperone activity *in vivo* using a novel RNA folding trap. *The EMBO Journal*, **18**, 3776-3782.
51. Arluison, V., Hohng, S., Roy, R., Pellegrini, O., Regnier, P. and Ha, T. (2007) Spectroscopic observation of RNA chaperone activities of Hfq in post-transcriptional regulation by a small non-coding RNA. *Nucleic Acids Research*, **35**, 999-1006.
52. Sukhodolets, M.V. and Garges, S. (2003) Interaction of *Escherichia coli* RNA polymerase with the ribosomal protein S1 and the Sm-like ATPase Hfq. *Biochemistry*, **42**, 8022-8034.
53. Mikulecky, P.J., Kaw, M.K., Brescia, C.C., Takach, J.C., Sledjeski, D.D. and Feig, A.L. (2004) *Escherichia coli* Hfq has distinct interaction surfaces for DsrA, *rpoS* and poly(A) RNAs. *Nat Struct Mol Biol*, **11**, 1206-1214.
54. Sun, X. and Wartell, R.M. (2006) *Escherichia coli* Hfq binds A18 and DsrA domain II with similar 2:1 Hfq6/RNA stoichiometry using different surface sites. *Biochemistry*, **45**, 4875-4887.
55. Ziolkowska, K., Derreumaux, P., Folichon, M., Pellegrini, O., Regnier, P., Boni, I.V. and Hajnsdorf, E. (2006) Hfq variant with altered RNA binding functions. *Nucleic Acids Research*, **34**, 709-720.
56. Arluison, V., Mutyam, S.K., Mura, C., Marco, S. and Sukhodolets, M.V. (2007) Sm-like protein Hfq: location of the ATP-binding site and the effect of ATP on Hfq--RNA complexes. *Protein Sci*, **16**, 1830-1841.
57. Vecerek, B., Rajkowitsch, L., Sonnleitner, E., Schroeder, R. and Bläsi, U. (2008) The C-terminal domain of *Escherichia coli* Hfq is required for regulation. *Nucleic Acids Research*, **36**, 133-143.
58. Gottesman, S., Squires, C., Pichersky, E., Carrington, M., Hobbs, M., Mattick, J.S., Dalrymple, B., Kuramitsu, H., Shiroza, T., Foster, T. *et al.* (1990) Conservation of the regulatory subunit for the Clp ATP-dependent protease in prokaryotes and eukaryotes. *Proceedings of the National Academy of Sciences of the United States of America*, **87**, 3513-3517.
59. Hengge-Aronis, R. (2002) Signal transduction and regulatory mechanisms involved in control of the sigma(S) (RpoS) subunit of RNA polymerase. *Microbiol Mol Biol Rev*, **66**, 373-395, table of contents.
60. Repoila, F., Majdalani, N. and Gottesman, S. (2003) Small non-coding RNAs, co-ordinators of adaptation processes in *Escherichia coli*: the RpoS paradigm. *Molecular Microbiology*, **48**, 855-861.

61. Majdalani, N., Hernandez, D. and Gottesman, S. (2002) Regulation and mode of action of the second small RNA activator of RpoS translation, RprA. *Molecular Microbiology*, **46**, 813-826.
62. Storz, G., Opdyke, J.A. and Zhang, A. (2004) Controlling mRNA stability and translation with small, noncoding RNAs. *Current Opinion in Microbiology*, **7**, 140-144.
63. Majdalani, N., Chen, S., Murrow, J., St John, K. and Gottesman, S. (2001) Regulation of RpoS by a novel small RNA: the characterization of RprA. *Molecular Microbiology*, **39**, 1382-1394.
64. Zhang, A., Altuvia, S., Tiwari, A., Argaman, L., Hengge-Aronis, R. and Storz, G. (1998) The OxyS regulatory RNA represses *rpoS* translation and binds the Hfq (HF-I) protein. *The EMBO Journal*, **17**, 6061-6068.
65. Sledjeski, D.D., Gupta, A. and Gottesman, S. (1996) The small RNA, DsrA, is essential for the low temperature expression of RpoS during exponential growth in *Escherichia coli*. *The EMBO Journal*, **15**, 3993-4000.
66. Majdalani, N., Cunning, C., Sledjeski, D., Elliott, T. and Gottesman, S. (1998) DsrA RNA regulates translation of RpoS message by an anti-antisense mechanism, independent of its action as an antisilencer of transcription. *Proceedings of the National Academy of Sciences of the United States of America*, **95**, 12462-12467.
67. Resch, A., Afonyushkin, T., Lombo, T.B., McDowall, K.J., Bläsi, U. and Kaberdin, V.R. (2008) Translational activation by the noncoding RNA DsrA involves alternative RNase III processing in the *rpoS* 5'-leader. *RNA*, **14**, 454-459.
68. Lease, R.A. and Woodson, S.A. (2004) Cycling of the Sm-like protein Hfq on the DsrA small regulatory RNA. *Journal of Molecular Biology*, **344**, 1211-1223.
69. Lipari, G. and Szabo, A. (1982) Model-free approach to the interpretation of nuclear magnetic resonance relaxation in macromolecules. 1. Theory and range of validity. *J. Am. Chem. Soc.*, **104**, 4546-4559.
70. Lipari, G. and Szabo, A. (1982) Model-free approach to the interpretation of nuclear magnetic resonance relaxation in macromolecules. 2. Analysis of experimental results. *J. Am. Chem. Soc.*, **104**, 4559-4570.
71. Clore, G.M., Driscoll, P.C., Wingfield, P.T. and Gronenborn, A.M. (1990) Analysis of the backbone dynamics of interleukin-1 beta using two-dimensional inverse detected heteronuclear 15N-1H NMR spectroscopy. *Biochemistry*, **29**, 7387-7401.
72. Miller, J.H. (1972) *Experiments in Molecular Genetics*. Cold Spring Harbor Laboratory, Cold Spring Harbor, NY.
73. Steiner, M., Lubitz, W. and Bläsi, U. (1993) The missing link in phage lysis of gram-positive bacteria: gene 14 of *Bacillus subtilis* phage phi 29 encodes the functional homolog of lambda S protein. *Journal of Bacteriology*, **175**, 1038-1042.
74. Muffler, A., Fischer, D. and Hengge-Aronis, R. (1996) The RNA-binding protein HF-I, known as a host factor for phage Qbeta RNA replication, is essential for *rpoS* translation in *Escherichia coli*. *Genes & Development*, **10**, 1143-1151.
75. Sonnleitner, E., Moll, I. and Bläsi, U. (2002) Functional replacement of the *Escherichia coli hfq* gene by the homologue of *Pseudomonas aeruginosa*. *Microbiology (Reading, England)*, **148**, 883-891.

76. Datsenko, K.A. and Wanner, B.L. (2000) One-step inactivation of chromosomal genes in *Escherichia coli* K-12 using PCR products. *Proceedings of the National Academy of Sciences of the United States of America*, **97**, 6640-6645.
77. Vecerek, B., Moll, I., Afonyushkin, T., Kaberdin, V. and Bläsi, U. (2003) Interaction of the RNA chaperone Hfq with mRNAs: direct and indirect roles of Hfq in iron metabolism of *Escherichia coli*. *Molecular Microbiology*, **50**, 897-909.
78. Sonnleitner, E., Schuster, M., Sorger-Domenigg, T., Greenberg, E.P. and Bläsi, U. (2006) Hfq-dependent alterations of the transcriptome profile and effects on quorum sensing in *Pseudomonas aeruginosa*. *Molecular Microbiology*, **59**, 1542-1558.
79. Lin-Chao, S. and Bremer, H. (1986) Effect of the bacterial growth rate on replication control of plasmid pBR322 in *Escherichia coli*. *Mol Gen Genet*, **203**, 143-149.
80. Resch, A., Tedin, K., Gründling, A., Mündlein, A. and Bläsi, U. (1996) Downstream box-anti-downstream box interactions are dispensable for translation initiation of leaderless mRNAs. *The EMBO Journal*, **15**, 4740-4748.

10 Curriculum Vitae

Hermann Hämmerle

Geburtsdatum:	09.07.1983
Geburtsort:	Feldkirch, Österreich
Staatsbürgerschaft:	Österreich
Adresse	Neustiftgasse 83/162, 1070 Wien
Telefonnummer	0043-664/2066538
E-mail	hermann.haemmerle@univie.ac.at

Präsenzdienst:

09/2001 - 03/2002	Walgaukaserne Bludesch, Jägerbataillon 23

Ausbildung:

1989 - 1993	Volksschule Rieden, Bregenz
1993 - 2001	Bundesgymnasium Blumenstraße, Bregenz neusprachlicher Zweig: - Englisch, Französisch, Latein - Wahlfach: Italienisch Matura: 16/06/2001
2002-2009	Universität Wien, Studienzweig Genetik / Mikrobiologie; Diplomarbeit am Department für Mikrobiologie und Immunologie; Labor: Prof. Dr. Udo Bläsi; „Functional Analysis of the *E. coli* Hfq_{G29A} Variant“ Diplomprüfung 07/2009